ELSEVIER

Remote Sensing of Environment 79 (2002) 23–29

Remote Sensing of Environment

www.elsevier.com/locate/rse

Variation in the projected surface area of suspended particles: Implications for remote sensing assessment of TSM

Ole Aarup Mikkelsen*

Institute of Geography, University of Copenhagen, Øster Voldgade 10, DK-1350 Copenhagen K, Denmark

Received 5 April 2001; received in revised form 12 May 2001; accepted 14 May 2001

Abstract

For decades, researchers have attempted to develop general algorithms for determining the concentration of total suspended matter (TSM) in coastal waters using remotely sensed measurements. On the basis of published work and empirical data, this paper demonstrates that reflectance and other optical parameters, such as the beam attenuation coefficient, are in reality, dependent on the projected surface area (PSA) of the suspended matter. The PSA is shown to be dependent on TSM, the volume concentration (VC), the particle size spectrum, and the mean effective density ($\Delta\rho$) of the suspended matter. The PSA is calculated for three different particle size spectra and it is shown that PSA can vary by up to three orders of magnitude at a constant value of TSM (if $\Delta\rho$ and the particle size spectrum change). Because reflectance and beam attenuation are de facto related to the PSA, determination of TSM from a reflectance or transmission measurement may potentially have an error of up to a factor of 10 due to variations in $\Delta\rho$ common in coastal and estuarine waters. If $\Delta\rho$ and the size spectrum of the suspended matter are known or can be estimated, it is possible to determine TSM from both types of measurement with better accuracy.

1. Introduction

Researchers have long been attempting to derive algorithms to determine the total suspended matter (TSM) concentration in coastal and estuarine waters using remotely sensed (RS) data. The majority of the proposed algorithms have been empirically derived and have usually been constructed by regression analysis of TSM against RS reflectance, $R(\lambda)$. Values of TSM have usually been determined by filtration of water samples obtained more or less simultaneously with the RS data. As a result of these empirical investigations, a number of equations relating $R(\lambda)$ to TSM have been derived for a variety of RS platforms (examples are given in Table 1). The number of empirical relations (and the differences between them) testifies to the difficulty of deriving an empirical algorithm for determining TSM that has regional, let alone global, validity.

Analytical models have also been developed (Kutser, Herlevi, Kallio, & Arst, 2001 and references therein). In these models, measured reflectance spectra are compared with modelled spectra. Reflectance spectra can be modelled if detailed knowledge about two inherent optical parameters, the absorption ($a(\lambda)$) and the backscattering ($b_b(\lambda)$) coefficients, is available. For any given wavelength, $a(\lambda)$ and $b_b(\lambda)$ vary as a function of a number of optically active in-water constituents including TSM, particle size, chl *a*, and gelbstoff (Strömbeck & Pierson, 2001; Stumpf & Pennock, 1989; Ulloa, Sathyendranath, & Platt, 1994). Reflectance spectra can be modelled for a range of values of the optically active parameters, and the modelled spectrum that compares best with the measured spectrum determined. It is then assumed that the values for, say, TSM, and chl *a* concentration in the measured spectrum are similar to those used in the modelled spectrum (Kutser et al., 2001). However, even when using this approach, measured and modelled values for TSM may still differ by a factor of between two and three (Kutser et al., 2001; Moore, Aiken, & Lavender, 1999).

One reason for these discrepancies was identified in a laboratory study by Bale, Tocher, Weaver, Hudson, and Aiken (1994). They showed that when TSM was constant, a 10-fold increase in $R(\lambda)$ could be found when the size spectrum of the suspended matter changed from

* Tel.: +45-3532-2545; fax +45-3532-2501.
E-mail address: oam@geogr.ku.dk (O.A. Mikkelsen).

0034-4257/02/$ – see front matter
PII: S0034-4257(01)00235-8

Table 1
Empirical relations between RS reflectance and TSM, derived for various RS platforms and environments

Author(s)	Relation	RS platform	Area
Matthews, Duncan, & Davison, 2001	$TSM = 3.39(R_{661}/R_{754}) - 2.6$	CASI	Bristol Channel, UK (best linear fit)
Matthews et al., 2001	$TSM = \exp(-0.739 + 0.929(R_{618}/R_{754}))$	CASI	Bristol Channel, UK (a single image, best exponential fit)
Matthews et al., 2001	$TSM = 44.22(R_{661}/R_{754}) - 84.7$	CASI	Norfolk coast, UK (best linear fit)
Matthews et al., 2001	$TSM = \exp[-5.356+(3.426(R_{575}/R_{747}))]$	CASI	Norfolk coast, UK (a single image, best exponential fit)
Matthews et al., 2001	$TSM = \exp[-5.920+(3.607(R_{618}/R_{754}))]$	CASI	Norfolk coast, UK (mosaic of three images, best exponential fit)
Matthews et al., 2001	$TSM = 23.96(R_{632}/R_{754}) - 34.27$	CASI	Bristol Channel and Norfolk coast, UK, combined
Robinson, Morris, & Dyer, 1999	$TSM = 3.505(R_{509}/R_{668})^{-2.726}$	CASI	Mouth of River Humber, UK
Forget & Ouillon, 1999	$R = 8.059 \log_{10}(TSM) + 0.947$[a]	Landsat TM	Rhône River, France
Forget & Ouillon, 1999	$R = 11.514 \log_{10}(TSM) + 0.249$[b]	Landsat TM	Rhône River, France
Forget & Ouillon, 1999	$R = 13.977 \log_{10}(TSM) - 5.509$[c]	Landsat TM	Rhône River, France
Dekker, Vos, & Peters, 2001	$TSM = 0.7581 \exp(61.683x)$[d]	Landsat TM	The Frisian Lakes, the Netherlands
Stumpf, 1988	$R = 0.081 \log_{10}(TSM) - 0.057$[e]	Landsat MSS	Chesapeake Bay, USA

[a] R = reflectance in percent in Landsat TM Band 1.
[b] R = reflectance in percent in Landsat TM Band 2.
[c] R = reflectance in percent in Landsat TM Band 3.
[d] x = average value for subsurface reflectance [$R(0-)$] in Landsat TM Bands 2 and 3.
[e] R = average value of reflectance in Landsat MSS Bands 5 and 6.

coarse (particles mainly >100 μm) to fine (particles mainly <10 μm). Bale et al. (1994) then introduced a new parameter, the net cross-sectional area, equivalent to the net projected surface area (PSA) of the suspended particle population. The PSA can be considered a combined measure of particle size distribution and concentration. Since small particles have a larger specific surface area than large particles, the PSA will be largest for smaller particles if TSM is kept constant. However, if an increase in TSM occurs simultaneously with a change in particle size from small to large, the PSA for the larger particles could equal the PSA for the small particles at the lower value of TSM. Bale et al. found an r^2 of .897 between PSA and $R(\lambda)$, strongly indicating that $R(\lambda)$ is in fact much more dependent on PSA than on TSM. The PSA, in turn, is dependent on the volume concentration (VC) and the size distribution of the suspended matter. Consequently, the relation between $R(\lambda)$ and TSM seems to be equivalent to the relation between the so-called beam attenuation coefficient (c) and the concentration and size distribution of suspended matter: c is known to vary dramatically with changes in the size distribution when TSM is almost constant (Baker & Lavelle, 1984; Mikkelsen & Pejrup, 2000).

This has serious implications for the derivation of TSM from RS data in coastal waters and estuaries, where the suspended in situ particle size and density is known to change by up to several orders of magnitude over very short time and space scales due to flocculation of suspended cohesive sediment particles, which are abundant in such waters (Eisma, 1986; Eisma et al., 1991; Kranck & Milligan, 1992; Mikkelsen & Pejrup, 2000). Therefore, the remainder of this paper is based on the hypothesis that the PSA can vary independently of TSM, due to changes in in situ particle size and density caused by flocculation (which do not, necessarily, cause a change in TSM). This would compromise derivation of TSM from RS data to some degree. Consequently, this paper sets out to investigate the nature of the relationship between PSA (as measured by a LISST-100 in situ laser) and TSM, together with the potential variation in PSA [hence, $R(\lambda)$ and c] in coastal waters.

2. Study areas and methods

2.1. Study areas

Measurements from four different coastal waters were obtained for this study (Fig. 1): A near coastal part of the North Sea (NS) off the Danish west coast, Horsens Fjord (HF) at the Danish East coast, the Øresund Sound (ØS) between Denmark and Sweden, and the Ebro River in Spain.

2.2. Methods

2.2.1. Particle measurements

At each study site, measurements of the beam attenuation coefficient (c), the VC, in situ particle size spectrum, and in situ mean grain size (D_M) of the suspended matter were obtained with a LISST-100 type C laser diffraction particle sizer. The LISST measures particle size by laser diffraction at 670 nm in 32 logarithmically spaced size classes in the range 2.5–500 μm. Details regarding LISST measurements and data analysis of LISST raw data can be found in Agrawal and Pottsmith (2000). Details regarding measurement and definition of c can be found in sources

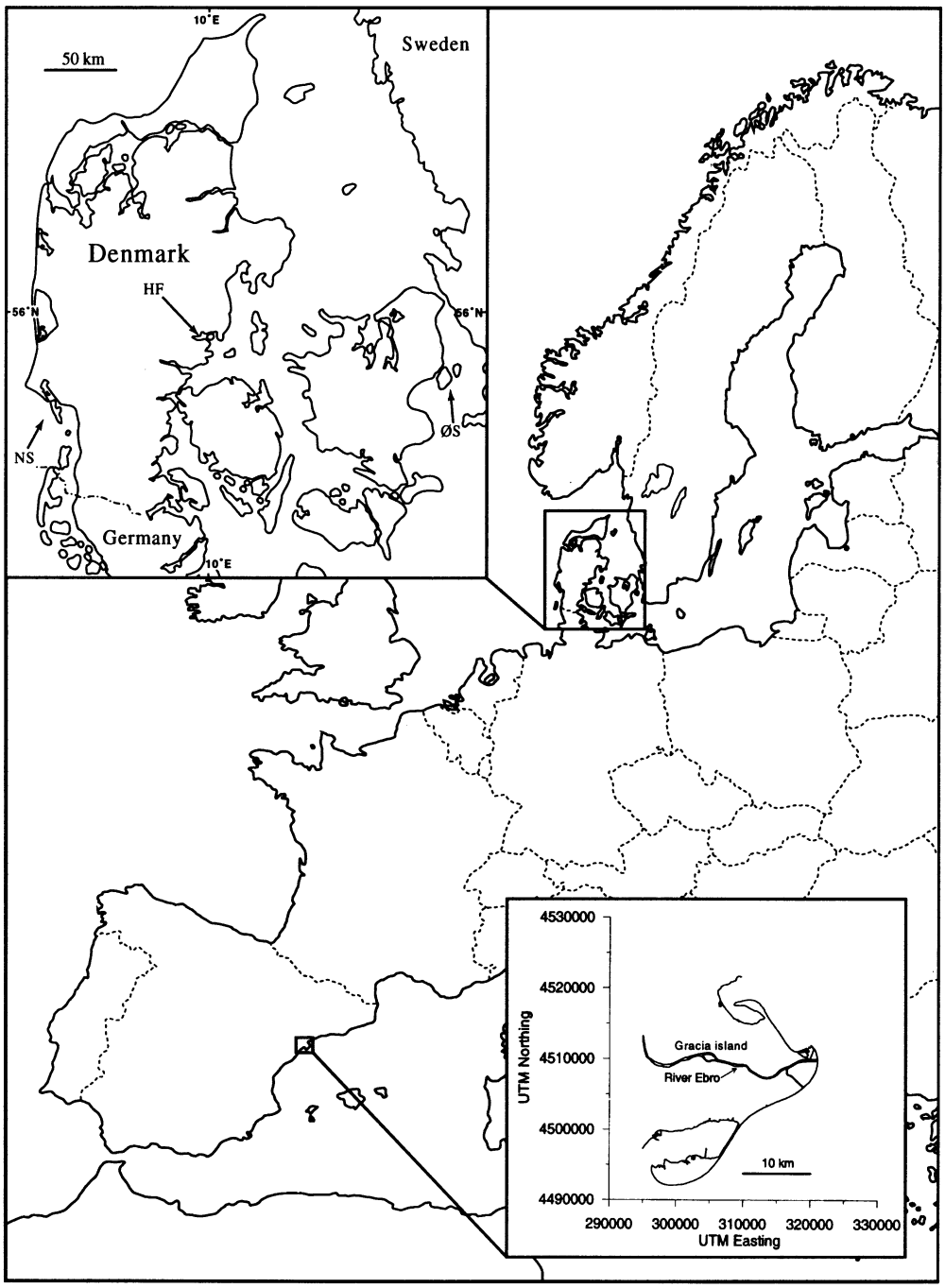

Fig. 1. Map of the study areas. The HF, the coastal part of the NS, the ØS in Denmark, and the Ebro River in Spain.

such as Baker and Lavelle (1984), Bartz, Zaneveld, and Pak (1978), Jerlov (1968), and Voss and Austin (1993). Suffice it to say, that c is the sum of absorption (a) plus scattering (b), i.e., $c = a + b$. Absorption is mainly caused by organic particles, while scattering is mainly caused by inorganic particles. In Case 2 waters, scattering by inorganic particles dominates over absorption and c has, therefore, often been used as a proxy for TSM in, for example, sediment transport studies (Jago & Jones, 1998; Riethmüller et al., 1988). In this study, LISST raw data were sampled and analysed according to the procedure described by Mikkelsen and Pejrup (2001).

2.2.2. Water sampling

Water samples for determination of TSM were taken with a 2-l water sampler at the same depth and time as the LISST measurements. TSM was determined by filtering the water samples through prefiltered, preweighed Millipore filters type HA (nominal retention diameter 0.45 μm), flushed three times with deionized water (in order to remove excess

salt from the filters and sediment), and oven-dried for 1 1/2 h at 65°C. Subsequently, the filters were allowed to adjust to room temperature for 1/2 h and weighed with a precision of 0.2 mg. Preweighed blanks followed the same procedure in order to determine whether the filters themselves gained or lost weight during the filtration.

2.2.3. Calculating the PSA

The PSA can be calculated from a LISST measurement of VC as follows.

If, in a size class i, the midpoint of the size class is denoted x_i, and assuming that all particles in the size class are spherical and of the same size (i.e., with a radius $x_i/2$), then the VC in the size class, VC_i, is given as (Eq. (1)):

$$VC_i = n_i \frac{4\pi(x_i/2)^3}{3} \iff n_i = \frac{3VC_i}{4\pi(x_i/2)^3} \quad (1)$$

where n_i is the number concentration of particles in size class i.

Each particle in size class i has a cross-sectional (projected) surface area, A_i, of (Eq. (2)):

$$A_i = \pi(x_i/2)^2 \quad (2)$$

Thus, the PSA of all particles in size class i, PSA_i, is the number concentration of particles in the size class times the PSA of each particle in the size class (Eq. (3)):

$$PSA_i = n_i A_i = \frac{3}{4}\frac{VC_i}{x_i/2} = 1.5\frac{VC_i}{x_i} \quad (3)$$

The total PSA for the suspended matter is calculated by summing the PSA for each of the 32 size classes (Eq. (4)):

$$PSA = \sum_{i=1}^{32} PSA_i = \sum_{i=1}^{32} 1.5\frac{VC_i}{x_i} \quad (4)$$

3. Results and discussion

3.1. Regression analysis

Linear regression analyses were carried out between PSA, D_M, VC, TSM, and c and between TSM and PSA (Fig. 2). The data from the Ebro River were excluded from the regression analysis, as they caused the entire data set ($n = 95$) to be positively skewed. Without the Ebro data, the data set ($n = 87$) had a normal distribution. Correlations were tested for significance at the 99% confidence interval using the Pearson Product–Moment Correlation Coefficient, r. All correlations except the one between VC and c were significant. However, the correlation between PSA and c is by far the best, having the narrowest confidence intervals and an r^2 of .883. As PSA is derived from the forward scattered laser light of the LISST-100, the good fit between PSA and c

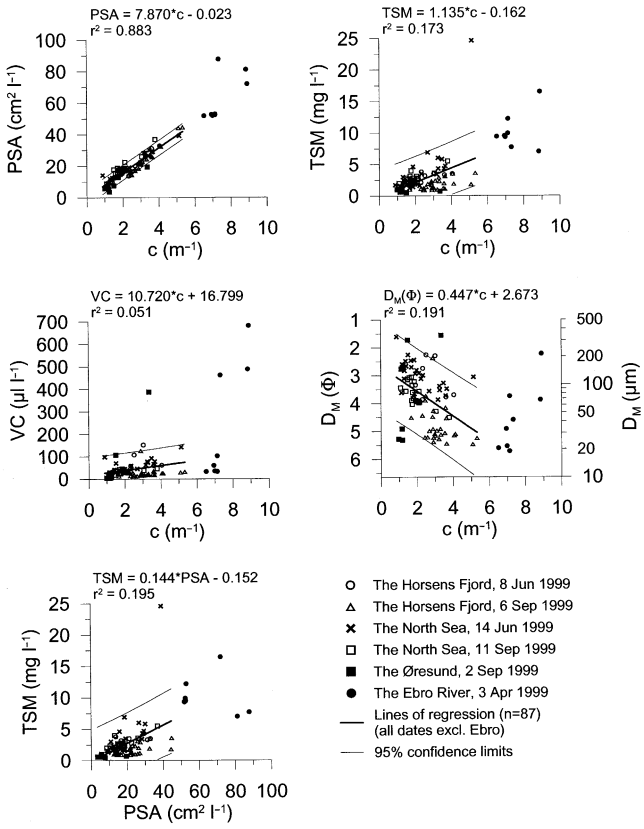

Fig. 2. Relationships between the PSA, TSM, VC, mean grain size (D_M), and the beam attenuation coefficient (c), together with the relationship between TSM and PSA, obtained in the study areas.

indicates that the attenuation is dominated by scattering from inorganic particles, not absorption from organic particles. It should be noted that the observed relationship between c and PSA is consistent with scattering theory (Baker & Lavelle, 1984; Bunt, Larcombe, & Jago, 1999; Spinrad, Zaneveld, & Kitchen, 1983; Zaneveld, Spinrad, & Bartz, 1982).

A negative relationship exists between D_M and c, i.e., c increases with decreasing D_M. This is in accordance with the findings of Mikkelsen and Pejrup (2000), who demonstrated that when TSM was almost constant, c was better (and negatively) correlated with D_M than with TSM. This is due to the fact that small particles have a larger specific surface area (i.e., surface area per unit mass) than larger particles. Since c is de facto dependent on surface area (cf. Fig. 2), small particles attenuate more light per unit mass than large particles. This effect is especially pronounced when a limited range in TSM is found together with a large variation in particle size, as in this study.

Also note that the potential for deriving TSM from PSA is poor, as the variation in PSA can only explain 20% of the variation in TSM (r^2=.195). This is due to the fact that fine-grained particles in seawater do not appear as single particles, but as aggregates (flocs), with a density much lower than the density of the constituent grains.

Other in-water optical parameters have also been found to be related to PSA, both empirically and theoretically. In a number of laboratory experiments, Bale et al. (1994) found a power relationship between PSA and $R(\lambda)$ of the form $PSA = 25.437R(\lambda)^{1.466}$ (r^2=.897), where $R(\lambda)$ was determined at 804 nm. The relationship between PSA and $R(\lambda)$ derived by Bale et al. is consistent with scattering theory and empirical observations (Forget, Ouillon, Lahet, & Broche, 1999; Stumpf, 1988; Stumpf & Pennock, 1989).

Thus, from knowledge of $R(\lambda)$ or c, PSA can be estimated with a high degree of accuracy. However, only if one is certain that TSM is well-correlated with PSA is it possible to deduce TSM from a measurement of $R(\lambda)$ or c. As shown in Fig. 2, this is not necessarily the case. In Section 3.2, the theoretical variation in PSA will be calculated and the nature of the relationship between PSA and TSM investigated.

3.2. Theoretical variation in PSA [hence, R(λ) and c]

In order to compute the PSA, is it necessary to know the VC and the frequency distribution (i.e., the size spectrum) of the suspended matter in situ (cf. Eq. (4)). The VC can be computed from TSM and the mean effective density ($\Delta\rho$) of the suspended particles. $\Delta\rho$ is defined as $\rho_F - \rho_W$, where ρ_F is the mean density of the suspended matter and ρ_W is the density of sea water. Mikkelsen and Pejrup (2000, 2001) derived a relationship between $\Delta\rho$, TSM, and VC of the form (Eq. (5)):

$$\Delta\rho \approx \frac{\mathrm{TSM}}{\mathrm{VC}} \iff \mathrm{VC} \approx \frac{\mathrm{TSM}}{\Delta\rho} \tag{5}$$

In order to choose realistic values of TSM and $\Delta\rho$ for the computation of VC, the variation in these parameters during the fieldwork periods in the study areas was examined (Table 2). It appears from the table that TSM varies between 0.5 and 25 mg l^{-1} and $\Delta\rho$ between 2 and 300 kg m^{-3}. This is in accordance with published data for similar environments (Fennessy, Dyer, & Huntley, 1994; Heffler, Syvitsski, & Asprey, 1991; Hill, Syvitski, Cowan, & Powell, 1998; McCave, 1975; Sternberg, Berhane, & Ogston, 1999). Therefore, VC was determined for five values of TSM (1, 3.2, 10, 32, and 100 mg l^{-1}) and five values of $\Delta\rho$ (3.2, 10, 32, 100, and 316 kg m^{-3}), yielding 25 values of VC for the 25 possible combinations of TSM and $\Delta\rho$.

Table 2
Range of variation in the concentration of TSM and effective density ($\Delta\rho$) for the four study areas

Location	Variation in TSM (mg l^{-1})	Variation in $\Delta\rho$ (kg m^{-3})
HF, 8 June 1999	2.1–3.8	18–166
HF, 6 September 1999	0.9–3.6	23–72
NS, 14 June 1999	1.2–24.6	17–174
NS, 11 September 1999	2.0–5.5	63–171
Ebro River, 3 April 1999	7.0–16.5	14–300
ØS, 2 September 1999	0.5–1.0	2–189

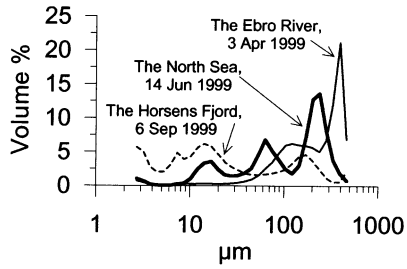

Fig. 3. Size spectra (frequency distributions) from the HF, NS, and Ebro River used for computation of the PSA (cf. Eq. (4)). Mean grain sizes for the three spectra are 24, 92, and 182 μm, respectively.

Two of the three size spectra chosen for the computation of the PSA are taken from Mikkelsen and Pejrup (2001) and were measured in the NS and HF, respectively. The remaining size spectrum was measured during the field campaign in the Ebro in Spain. The spectra are shown in Fig. 3. Also indicated in Fig. 3 is D_M for each spectrum.

From the frequency distribution, the VC in each size class (VC_i) for each of the three spectra was calculated as $f(i)$VC, where $f(i)$ is the relative frequency in size class i. For each of the three spectra, VC_i was determined for all 32 size classes for a given value of VC, and the PSA was subsequently calculated for each spectra according to Eq. (4). Finally, PSA as a function of TSM and $\Delta\rho$ was plotted for each of the three spectra (Fig. 4). Note that computed values for PSA exceeding 100 $cm^2\ l^{-1}$ have been excluded from Fig. 4, as the values actually measured for PSA in this study were below 100 $cm^2\ l^{-1}$ (Fig. 2).

From Fig. 4, it is clear that a wide range of values for PSA can occur for a constant value of TSM. For example, in the Ebro, changing $\Delta\rho$ meant that PSA could vary by a factor of 100 (between 0.5 and 54 $cm^2\ l^{-1}$) for a constant value of TSM of 1 mg l^{-1}. Similarly, a constant value of PSA could be obtained with widely varying TSM. This can

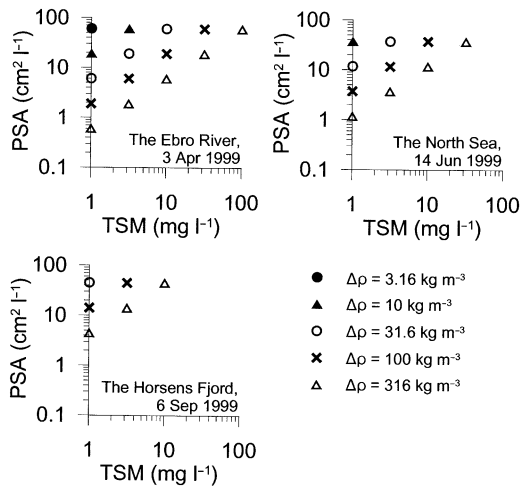

Fig. 4. Plots showing the relationships between the PSA, TSM, and the effective density ($\Delta\rho$) for each of the three spectra in Fig. 3. PSA is plotted in the range between 1 and 100 $cm^2\ l^{-1}$ only, as this is the variation in PSA found in the study areas (cf. Fig. 2).

also be demonstrated with the results from the Ebro, where a PSA of 54 $cm^2\ l^{-1}$ could be obtained for TSM varying by more than two orders of magnitude (from 1 to 100 mg l^{-1}), if $\Delta\rho$ of the suspended matter varied between 3.16 and 316 kg m^{-3}. As mentioned earlier, this range of variation in $\Delta\rho$ and TSM is realistic for coastal waters (cf. Table 2). Hence, the calculated variation in PSA must also be considered realistic.

The influence of the size spectrum can also be evaluated from Fig. 4. Compare, for example, the results from HF with the Ebro results. It is obvious from the size spectra in Fig. 3 that the suspended matter in HF was markedly finer than that in the Ebro. The influence of this difference is easily seen in Fig. 4, where the values for PSA in HF are displaced almost one order of magnitude for constant TSM and $\Delta\rho$ relative to PSA in Ebro. For example, for TSM = 10 mg l^{-1} and $\Delta\rho$ = 316 kg m^{-3}, PSA in HF would be 45 $cm^2\ l^{-1}$, while it would be 6 $cm^2\ l^{-1}$ in the Ebro.

The size spectrum from the NS has a D_M of 92 μm and so lies between the spectra from the Ebro and HF (cf. Fig. 3). This is also seen in the results of the calculation of PSA where, for constant values of TSM and $\Delta\rho$, PSA for the NS spectrum takes on values intermediate to those from the Ebro and HF.

3.3. Probable variation in PSA [hence, R(λ) and c]

The question then arises: For a given environment, how large a variation in PSA [hence, $R(\lambda)$ and c] can be expected? The range in TSM considered here is realistic for almost all coastal and some estuarine waters. TSM may even reach values of several thousand milligrams per liter in estuarine waters. In energetic waters such as estuaries, the internal shearing forces in the water tend to break down loosely bound, low-density flocs and restructure them into more compact ones with a higher density. Consequently, a variation of $\Delta\rho$ between 100 and approximately 300 kg m^{-3} is highly realistic for energetic, turbid estuarine waters, where the majority of the flocs consist of inorganic mineral grains (Fennessy et al., 1994; Winterwerp, 1999). This variation in $\Delta\rho$ causes a variation in PSA of a factor of 3 for any given value of TSM (cf. Fig. 4). In coastal waters, where a larger proportion of the suspended matter consists of organic matter of low density, slightly lower values of $\Delta\rho$ varying within one order of magnitude, say 10–100 kg m^{-3}, are quite realistic (Alldredge & Gotschalk, 1988; Mikkelsen & Pejrup, 2001). This corresponds to a variation in PSA of a factor of 10 for any given value of TSM (cf. Fig. 4). Thus, one should expect a variation in PSA [hence, $R(\lambda)$ and c] between a factor of 3 and approximately 10 for estuarine and coastal waters for any value of TSM. The implication of this is that one has to accept an error of up to a factor of 10 when using $R(\lambda)$ or c to derive values of TSM from remote sensing or transmissometer data. This is in agreement with published data (Baker & Lavelle, 1984; Matthews et al., 2001; Van Raaphorst, Philippart, Smit, Dijkstra, & Malschaert, 1998). It should be noted that this range of error only applies if an empirically derived relationship is used under different conditions compared to the time of calibration, i.e., is transferred from the area where it was developed to another area (or to the same area, but at a later time) where no TSM data exists for (re)calibration/validation. TSM can usually be determined within a factor of two for the data set that was used to develop an empirical algorithm (Forget & Ouillon, 1999; Stumpf & Pennock, 1989). As PSA varies as a function of TSM, $\Delta\rho$, and the in situ particle size spectrum, it is possible to reduce the variation between PSA and TSM if information regarding $\Delta\rho$ and the in situ particle size spectrum exists or can be modelled.

4. Conclusions

(1) The net cross-sectional area (PSA) of suspended particulate matter can be calculated using a LISST-100, as described above.

(2) The PSA is dependent on the VC and the in situ particle size distribution of the suspended matter.

(3) Own data and literature studies show that both $R(\lambda)$ and the beam attenuation coefficient, c, are highly dependent on PSA.

(4) The absence of any clear correlation between PSA and TSM means that TSM derived from RS data or transmissometer data can be erroneous.

(5) The error has been calculated and may be as large as a factor of 10.

(6) The size of the error can be reduced if information regarding the in situ particle size spectrum and $\Delta\rho$ exists (or can be modelled).

Acknowledgments

This paper was prepared as part of the Danish Environmental Monitoring of Coastal Waters (DECO) and Preparation and Integration of Analysis Tools towards Operational Forecast of Nutrients in Estuaries of European Rivers (PIONEER) projects. The DECO project was financed by grant no. 9600667 from the Danish Space Board, the Danish Natural Science Research Council, the Danish Technical Research Council, and the Danish Agricultural and Veterinary Research Council, while the PIONEER project was financed by the EU MAST III contract no. MAS3-CT98-0170. Lotte Nyborg and Thorbjørn J. Andersen (Institute of Geography) both participated in various parts of the fieldwork, for which I am grateful. Earlier versions of this paper benefited from comments made by Thomas T. Nielsen, Diego A. Berastegui, Michael S. Rasmussen, and Morten Pejrup. The comments of two anonymous reviewers are appreciated.

References

Agrawal, Y. C., & Pottsmith, H. C. (2000). Instruments for particle size and settling velocity observations in sediment transport. *Marine Geology*, *168*, 89–114.

Alldredge, A. L., & Gotschalk, C. (1988). In situ settling behavior of marine snow. *Limnology and Oceanography*, *33*, 339–351.

Baker, E. T., & Lavelle, J. W. (1984). The effect of particle size in the light attenuation coefficient of natural suspensions. *Journal of Geophysical Research*, *89*, 8197–8203.

Bale, A. J., Tocher, M. D., Weaver, R., Hudson, S. J., & Aiken, J. (1994). Laboratory measurements of the spectral properties of estuarine suspended particles. *Netherlands Journal of Aquatic Ecology*, *28*, 237–244.

Bartz, R. B., Zaneveld, J. R. V., & Pak, H. (1978). A transmissometer for profiling and moored observations in water. In: M. B. White, & R. E. Stevenson (Eds.), *Proceedings of the Society of Photo-Optical Instrumentation Engineers Ocean optics V*, (vol. 160, pp. 102–108). Bellingham: Society of Photo-Optical Instrumentation Engineers.

Bunt, J. A. C., Larcombe, P., & Jago, C. F. (1999). Quantifying the response of optical backscatter devices and transmissometers to variations in suspended particulate matter. *Continental Shelf Research*, *19*, 1199–1220.

Dekker, A. G., Vos, R. J., & Peters, S. W. M. (2001). Comparison of remote sensing data, model results and in situ data for total suspended matter (TSM) in the southern Frisian lakes. *The Science of the Total Environment*, *268*, 197–214.

Eisma, D. (1986). Flocculation and de-flocculation of suspended matter in estuaries. *Netherlands Journal of Sea Research*, *20*, 183–199.

Eisma, D., Bernard, P., Cadeé, G. C., Ittekkot, V., Kalf, J., Laane, R., Martin, J. M., Mook, W. G., van Put, A., & Schuhmacher, T. (1991). Suspended-matter particle size in some west-european estuaries: Part I. Particle-size distribution. *Netherlands Journal of Sea Research*, *28*, 193–214.

Fennessy, M. J., Dyer, K. R., & Huntley, D. A. (1994). INNSEV: an instrument to measure the size and settling velocity of flocs in situ. *Marine Geology*, *117*, 107–117.

Forget, P., & Ouillon, S. (1999). Surface suspended matter off the Rhone river mouth from visible satellite imagery. *Oceanologica Acta*, *21*, 739–749.

Forget, P., Ouillon, S., Lahet, F., & Broche, P. (1999). Inversion of reflectance spectra of nonchlorophyllous turbid coastal waters. *Remote Sensing of Environment*, *68*, 264–272.

Heffler, D. E., Syvitski, J. P. M., & Asprey, K. W. (1991). The floc camera assembly. In: J. P. M. Syvitski (Ed.), *Principles, methods, and application of particle size analysis* (pp. 209–221). New York: Cambridge Univ. Press.

Hill, P. S., Syvitski, J. P. M., Cowan, E. A., & Powell, R. D. (1998). In situ observations of floc settling velocities in Glacier Bay, Alaska. *Marine Geology*, *145*, 85–94.

Jago, C., & Jones, S. E. (1998). Observation and modelling of the dynamics of benthic fluff resuspended from a sandy bed in the southern North Sea. *Continental Shelf Research*, *18*, 1255–1282.

Jerlov, N. G. (1968). *Optical oceanography*. Amsterdam: Elsevier.

Kranck, K., & Milligan, T. G. (1992). Characteristics of suspended particles at an 11-hour anchor station in San Francisco Bay, California. *Journal of Geophysical Research*, *97*, 11373–11382.

Kutser, T., Herlevi, A., Kallio, K., & Arst, H. (2001). A hyperspectral model for interpretation of passive optical remote sensing data from turbid lakes. *The Science of the Total Environment*, *268*, 47–58.

Matthews, A. M., Duncan, A. G., & Davison, R. G. (2001). Error assessment of validation techniques for estimating suspended particulate matter concentration from airborne multispectral imagery. *International Journal of Remote Sensing*, *22*, 449–469.

McCave, I. N. (1975). Vertical flux of particles in the ocean. *Deep-Sea Research*, *22*, 491–502.

Mikkelsen, O. A., & Pejrup, M. (2000). In situ particle size spectra and density of particle aggregates in a dredging plume. *Marine Geology*, *170*, 443–459.

Mikkelsen, O. A., & Pejrup, M. (2001). The use of a LISST-100 laser particle sizer for in-situ estimates of floc size, density and settling velocity. *Geo-Marine Letters*, *20*, 187–195 (DOI: 10.1007/s003670100064).

Moore, G. F., Aiken, J., & Lavender, S. J. (1999). The atmospheric correction of water colour and the quantitative retrieval of suspended particulate matter in Case II waters: application to MERIS. *International Journal of Remote Sensing*, *20*, 1713–1733.

Riethmüller, R., Fanger, H.-U., Grabemann, I., Krasemann, H. L., Ohm, K., Böning, J., Neumann, L. J. R., Lang, G., Markofsky, M., & Schubert, R. (1988). Hydrographic measurements in the turbidity zone of the Weser Estuary. In: J. Dronkers, & W. van Leussen (Eds.), *Physical processes in estuaries* (pp. 332–344). Berlin: Springer-Verlag.

Robinson, M.-C., Morris, K. P., & Dyer, K. R. (1999). Deriving fluxes of suspended particulate matter in the Humber Estuary, UK, using airborne remote sensing. *Marine Pollution Bulletin*, *37*, 155–163.

Spinrad, R. W., Zaneveld, J. R. V., & Kitchen, J. C. (1983). A study of the optical characteristics of the suspended particles in the benthic nepheloid layer of the Scotian Rise. *Journal of Geophysical Research*, *88*, 7641–7645.

Sternberg, R. W., Berhane, I., & Ogston, A. S. (1999). Measurement of size and settling velocity of suspended aggregates on the northern California continental shelf. *Marine Geology*, *154*, 43–53.

Strömbeck, N., & Pierson, D. C. (2001). The effects of variability in the inherent optical properties on estimations of chlorophyll a by remote sensing in Swedish freshwaters. *The Science of the Total Environment*, *268*, 123–137.

Stumpf, R. P. (1988). Sediment transport in Chesapeake Bay during floods: analysis using satellite and surface observations. *Journal of Coastal Research*, *4*, 1–15.

Stumpf, R. P., & Pennock, J. R. (1989). Calibration of a general optical equation for remote sensing of suspended sediments in a moderately turbid estuary. *Journal of Geophysical Research*, *94*, 14363–14371.

Van Raaphorst, W., Philippart, C. J. M., Smit, J. P. C., Dijkstra, F. J., & Malschaert, J. F. P. (1998). Distribution of suspended particulate matter in the North Sea as inferred from NOAA/AVHRR reflectance images and in situ observations. *Journal of Sea Research*, *39*, 197–215.

Voss, K. J., & Austin, R. W. (1993). Beam-attenuation measurement error due to small-angle scattering acceptance. *Journal of Atmospheric and Oceanic Technology*, *10*, 113–121.

Ulloa, O., Sathyendranath, S., & Platt, T. (1994). Effect of the particle-size distribution on the backscattering ratio in seawater. *Applied Optics*, *33*, 7070–7077.

Winterwerp, J. C. (1999). *On the dynamics of high-concentrated mud suspensions*. PhD thesis, Technical University of Delft, 172 pp.

Zaneveld, J. R. V., Spinrad, R. W., & Bartz, R. (1982). An optical settling-tube for the determination of particle-size distributions. *Marine Geology*, *49*, 357–376.